Journal of Materials Chemistry B

PAPER

View Article Online
View Journal | View Issue

Cite this: J. Mater. Chem. B, 2014, 2, 6634

A benzothiazole-based sensor for pyrophosphate (PPi) and ATP: mechanistic insight for anion-induced ESIPT turn-on†

Junfeng Wang,[a] Xiumin Liu[a] and Yi Pang*[ab]

Received 7th July 2014
Accepted 5th August 2014

DOI: 10.1039/c4tb01109k

www.rsc.org/MaterialsB

A benzothiazole derivative **2** bearing two 2,2′-dipicolylamine (DPA) groups was examined for its zinc-binding and subsequent anion sensing properties. The study revealed the anion sensing mechanism of polyphosphate anions *via* sequential binding to two zinc centers, on the basis of both ^{1}H NMR and mass spectral evidence. The mechanistic insight would provide valuable information for the future design of new excited state intramolecular proton transfer (ESIPT) sensors. In addition, the zinc complex exhibited solvent-switchable selectivity, responding to pyrophosphate (PPi) in EtOH and adenosine 5′-triphosphate (ATP) in water.

The design of fluorescent chemosensors for biologically relevant anions remains a challenging topic.[1–3] This is due to the lack of a general design principle that can reliably translate an anion-binding event into a large fluorescent signal response.[4] One of the most successful strategies for anion recognition has been the use of coordination complexes that bear one or two vacant coordination sites for binding anionic guests.[5–8] This strategy can be realized *via* a proper arrangement of two zinc centers, which can selectively bind anions such as pyrophosphate (PPi)[9–16] and adenosine 5′-triphosphate (ATP).[4,17,18] However, this binding pattern usually induced little spectral shift in the fluorescence signal, which lowers the sensitivity and hampers their practical applications. An ideal fluorescent sensor should exhibit a great fluorescence turn-on with a large spectral shift, in order to minimize the interference from the free dye.[19]

The excited state intramolecular proton transfer (ESIPT) has been shown to be an attractive mechanism, as the ESIPT ON–OFF could induce a large spectral shift.[20] A few attempts have been made to incorporate the ESIPT mechanism in the PPi sensor scheme on the basis of either a mononuclear zinc complex (**1a-Zn**),[21] which responds to diphosphate ions ($H_2P_2O_7^{2-}$ and ADP), or binuclear zinc complex (**1b-Zn**, where R = "–CH_2DPA–Zn").[22] Herein, we report the ESIPT properties of sensor **2**, a thiazole analogue of **1b**, where the sulfur heteroatom perturbs the ESIPT and related chemical processes. Interestingly, the sensor exhibited solvent-switchable recognition for pyrophosphate (in alcohol) and ATP (in water). The anion recognition is accompanied by a large spectral shift (~95 nm shift from blue to green), which is useful for naked eye detection. In addition, the heteroatom substitution makes the two zinc binding sites in **2** distinguishable from each other, thereby allowing close examination of the sensing mechanism step-by-step. This result led to a better understanding about the ESIPT turn-on (Scheme 1).

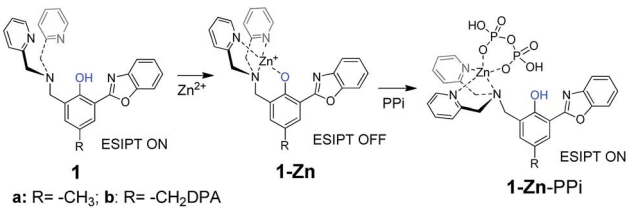

Scheme 1 Structure of **1**, the zinc complexes and the ESIPT OFF–ON switch induced by H_2PPi.

Formation of the ligand–zinc complex

Ligand **2** was synthesized as a light yellow syrup-like oil by using a similar strategy with a modified procedure (see ESI, Scheme S1†).[21,22] Our initial attention was paid to the process of zinc binding-induced ESIPT turning-off, by addition of different equiv. of $Zn(NO_3)_2$ to **2**. When the first equiv. of Zn^{2+} was added, the absorption peak (λ_{max} = 343 nm) was red-shifted to λ_{max} = 367 nm, as a consequence of deprotonation Ph–OH → Ph–O^- (Fig. 1a).[21,22] The observation clearly indicated that the first Zn^{2+} predominantly bound to "the site I" to disable the ESIPT, which caused the blue fluorescent shift with great fluorescence turn-on (Fig. 1b). The second equiv. of Zn^{2+} induced nearly no

[a]Department of Chemistry, The University of Akron, Akron, Ohio 44325, USA. E-mail: yp5@uakron.edu

[b]Maurice Morton Institute of Polymer Science, The University of Akron, Akron, Ohio 44325, USA

† Electronic supplementary information (ESI) available. See DOI: 10.1039/c4tb01109k

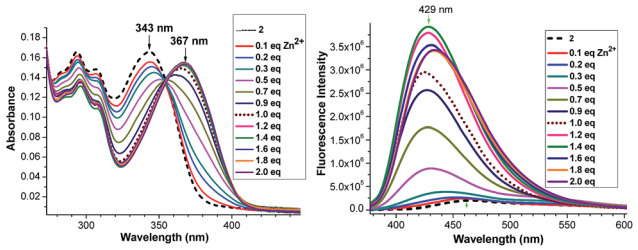

Fig. 1 UV-vis (left) and fluorescence (right) titration of **2** (10 μM) upon addition of different equiv. of Zn^{2+} in EtOH.

spectral shift in absorption, as the Zn^{2+} cation was bound to the second DPA group, resulting in the formation of complex **4** (Scheme 2). The binding of the second Zn^{2+} further increased the fluorescence, which is consistent with the previous data (by removing the weak PET effect from DPA).[21] Fluorescence quantum yields of **2** ($\phi_{fl} = 0.01$) and **4** ($\phi_{fl} = 0.17$) were calculated by using quinine sulfate as the reference.

^{1}H NMR titration further confirmed the assumption. The proton signals at ~8.5 ppm were attributed to two overlapping doublets from the characteristic pyridine protons H_a and H_a', which are associated with different zinc binding sites in **2**. The addition of the first equiv. Zn^{2+} only caused a downfield shift of H_a at the site I (from 8.53 to 8.70), and the second equiv. Zn^{2+} gradually induced a downfield shift of H_a' at the site II (from 8.56 to 8.60) (Fig. 2). Similarly, the same trend was observed from the mass experiments (Fig. S1, ESI†). Upon addition of the first equiv. of Zn^{2+}, the signal of ligand **2** (TOF-MS-ES$^+$ at peaks $[2 + H^+]^+ = 650.3146$ and $[2 + Na^+]^+ = 672.2971$) almost disappeared (ESI Fig. S1†) with the formation of a new peak corresponding to $[2 + Zn^{2+} - H^+]^+ = 712.2447$. Two-dimensional ESI-traveling wave ion mobility mass spectrometry (TWIM-MS) further revealed that the mass peak at $m/z = 712$ included two signals with drift times at 2.89 ms and 4.96 ms, which were assumed to be **3b** and **3a**, respectively (Fig. 3). It appeared that the mono-charged complex **3a** with the drift time of 4.96 ms was

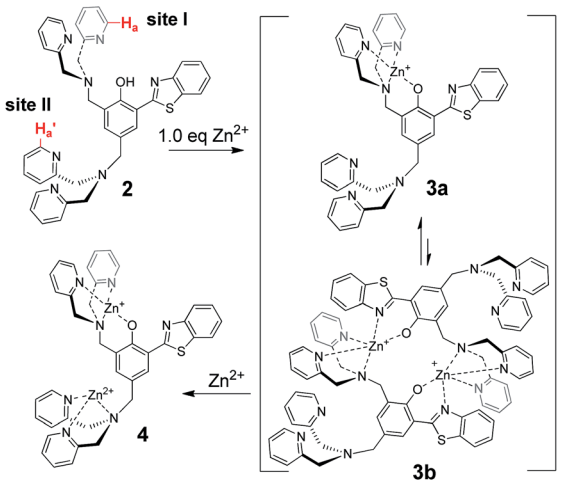

Scheme 2 Structure of **2** with two different zinc-binding sites (I and II), and its zinc complex formation.

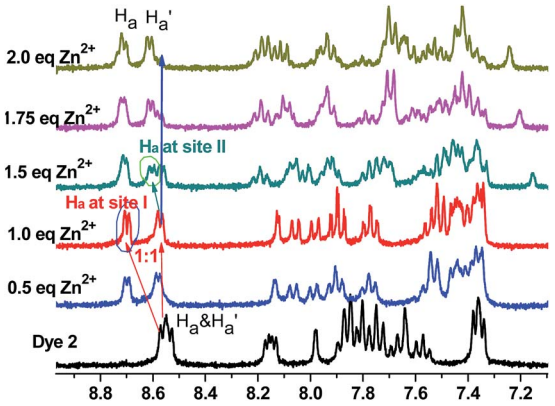

Fig. 2 ^{1}H NMR titration of **2** upon addition of different equiv. of Zn^{2+} in CD_3OD.

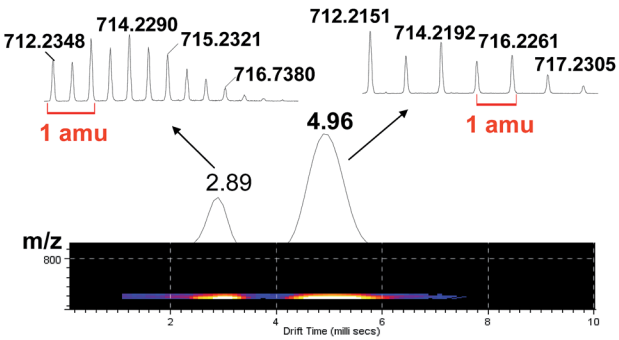

Fig. 3 Two-dimensional ESI TWIM MS plot for *m/z* at 712. Ion mobility separation was effected using a traveling wave height of 9 V and a traveling wave velocity of 350 m s^{-1}. The precursor ion from *m/z* at 712 gives rise to signals at 2.89 and 4.96 ms; on the basis of the isotope patterns observed, the signals at 2.89 and 4.96 ms agree well with $[(2 + Zn^{2+})_2 - 2H^+]^{2+}$ (**3b**) and $[2 + Zn^{2+} - H^+]^+$ (**3a**).

predominant. Upon addition of the second equiv. Zn^{2+}, the signals of complex **3** gradually disappeared, and the di-zinc complex **4** was detected as the predominant species with three positive charges: $[2 + 2Zn^{2+} - H^+]^{3+} = 258.7352$ (Fig. S2, ESI†). All the data pointed to that the zinc complex with four coordination (at the site I) are easier to form than that with three coordination (at the site II).

Binding to phosphate anions

The anion response of the resulting zinc complex **4** was examined by addition of 5.0 equiv. of different anions in EtOH. Much to our delight, **4** showed very good selectivity toward H_2PPi, giving the ESIPT turn-on with bright green emission (Fig. 4a and c). Interestingly, **4** showed selectivity toward H_2ATP over the other anions in aqueous (Fig. 4b and c). The mass spectra from the solution of "**4** + H_2PPi" in EtOH detected the major species with *m/z* = 952.1031 and 974.1014, which matched with the isotope patterns for $[5 + H^+]^+ = 952.0404$ ($C_{39}H_{36}N_7O_8P_2SZn_2$) and $[5 + Na^+]^+ = 974.0224$ ($C_{39}H_{36}N_7NaO_8P_2SZn_2$) (ESI† Fig. S10).

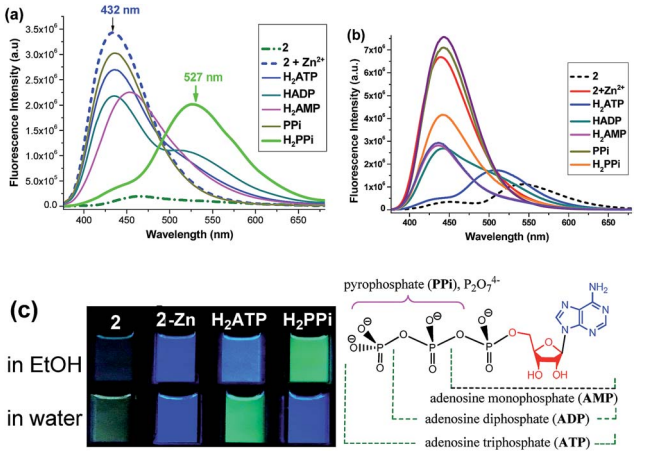

Fig. 4 Fluorescence response of Zn complex **4** (10 μM) with different anions (50 μM) in ethanol (a) and different anions (2 mM) in water (b), while the dye was excited at the isosbestic point ~357 nm. The fluorescence image (c) shows the response of **4** to various phosphate anions in ethanol (top) and DI water (bottom).

The observation pointed to the formation of **5**, which is essential to turn on the ESIPT.

A clear differentiation of ^{1}H NMR signals at two different zinc binding sites allowed us to further examine the details of pyrophosphate binding. Upon addition of H_2PPi to the zinc complex **4** (*i.e.* **2**–Zn_2), both H_a and H_a' (at 8.6 and 8.7 ppm) disappeared simultaneously to form a new broad peak at ~8.8 ppm. The spectral shift suggests that H_2PPi was binding to both site I (from the H_a shift) and site II (from H_a' shift) (Fig. 5a). The observation supports the formation of **5** (Scheme 3), which was the key for the ESIPT turn-on mechanism. The PPi adduct **6** might also be possible, since the PPi anion can bind to a mononuclear zinc center.[21] The control experiment was carried out by reaction of zinc complex **3a** with PPi, which would give **7**. The ^{1}H NMR of **7** showed that the H_a at site I would have a different pattern if PPi was bonded to only one zinc cation (Fig. 5b). The result thus consistently pointed to the formation of **5**, and ruled out the presence of **6** (Scheme 3).

As seen in Fig. 4b and c, the zinc complex showed an interesting response to H_2ATP in aqueous solution (pH ≈ 4.0 for 2 mM H_2ATP). The mass spectrum of the aqueous solution detected the formation of a major species at m/z = 1281.2192 and 1303.2233, which matched with the isotope pattern of intermediates $[\mathbf{8} + H^+]^+$ and $[\mathbf{8} + Na^+]^+$ respectively (Fig. 6; ESI Fig. S3, S11†), also showing the binding of H_2ATP to both binding sites I and II.

The stability of complex **4** was further examined in buffered aqueous at different pH values. The study revealed that complex **4** was quite stable in buffered aqueous at different pH values (ranges from pH = 4.7 to 7.7) (Fig. 7). When pH = 4.7, the ESIPT turn-on could be accomplished by H_2ATP (Fig. 8). The selectivity of **4** to phosphate anions was examined. The result showed that H_2ATP exhibited a stronger tendency to turn-on ESIPT over other phosphate anions such as H_2PPi (Fig. 9), revealing the same trend as observed in DI water

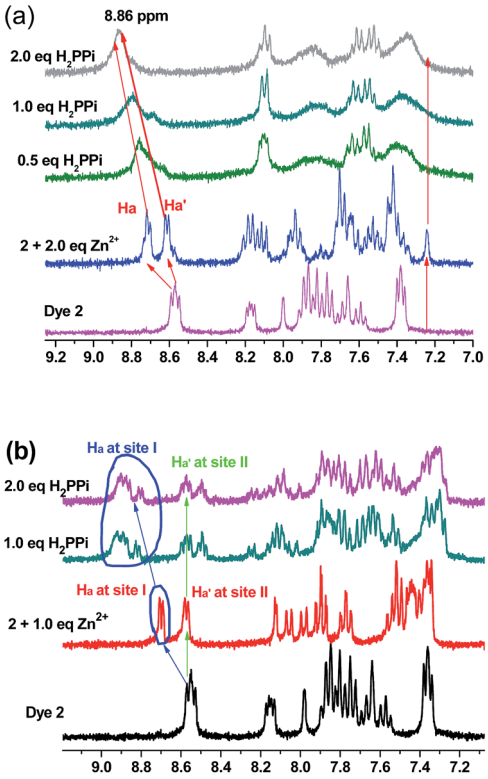

Fig. 5 ^{1}H NMR spectra of **4** (a) and **3** (b) upon addition of H_2PPi in CD_3OD.

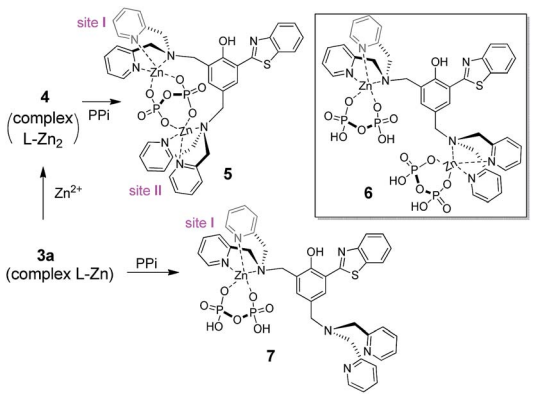

Scheme 3 Possible formation of PPi adducts from zinc complexes.

(Fig. 4b). The reversal of selectivity in different solvents, *i.e.* H_2PPi in EtOH and H_2ATP in water (or acidic buffer), showed that the anion binding-induced ESIPT turn-on was quite sensitive to the solvent environment, which should be further examined. Clearly, the current sensor worked better under the acidic conditions, as the ESIPT turn-on requires an H^+ to generate the phenol: Ph–O^- + H^+ → Ph–OH.

In conclusion, benzothiazole derivative **2** bearing two DPA groups was examined for its zinc-binding and subsequent anion sensing properties. The binuclear zinc complex was formed *via* sequential zinc chelating at two different DPA groups. Spectral data analysis, including UV-vis, fluorescence, ^{1}H NMR and ESI-

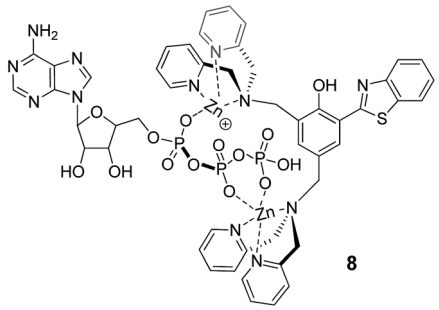

Fig. 6 Possible formation of H_2ATP adducts from zinc complexes in water.

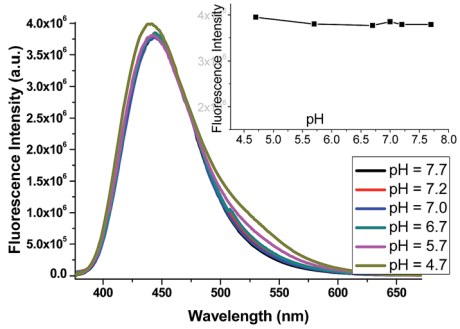

Fig. 7 Fluorescence intensity of **4** in PBS buffer at different pH values. The inset plots the stability of the complex at different pH values (4.7–7.7).

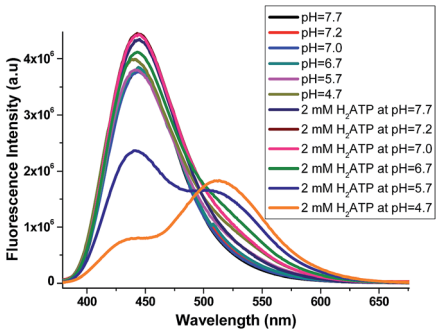

Fig. 8 Fluorescence intensity of **4** (10 μM) in PBS buffer at different pH values, upon addition of 2 mM of H_2ATP.

Mass spectra, suggested that the polyphosphate anions were likely binding to two zinc centers during the sensing process. Unexpectedly, the zinc complex **4** showed very good selectivity toward H_2PPi in EtOH and H_2ATP in H_2O, respectively, over the other anions. The intriguing selectivity is accompanied by ESIPT turn-on (from blue color to green color) to generate a large spectral shift, making it possible for naked-eye detection. The solvent-switchable selectivity suggests that the ESIPT probe is quite sensitive to the conditions used, and has the potential to differentiate structurally similar anions (PPi and ATP). The study also revealed the anion sensing mechanism, on the basis of both ^1H NMR and mass spectral evidence. The mechanistic

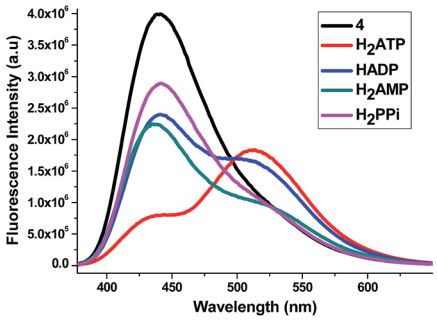

Fig. 9 Fluorescence intensity of **4** (10 μM) in PBS buffer (pH = 4.7), upon addition of 2 mM of phosphate anions.

insight would provide a useful guide for the future design of new ESIPT sensors.

Acknowledgements

This work was supported by National Institute of Health (Grant no: 1R15EB014546-01A1). We also thank the Ohio Department of Development and Coleman endowment from the University of Akron for partial support.

Notes and references

1 E. J. O'Neil and B. D. Smith, *Coord. Chem. Rev.*, 2006, **250**, 3068.
2 R. Martínez-Máñez and F. Sancenon, *Chem. Rev.*, 2003, **103**, 4419.
3 P. D. Beer and P. A. Gale, *Angew. Chem., Int. Ed.*, 2001, **40**, 486.
4 A. Ojida, I. Takashima, T. Kohira, H. Nonaka and I. Hamachi, *J. Am. Chem. Soc.*, 2008, **130**, 12095.
5 P. D. Beer and S. R. Bayly, *Top. Curr. Chem.*, 2005, **255**, 125.
6 J. W. Steed, *Chem. Soc. Rev.*, 2009, **38**, 506.
7 E. J. O'Neil and B. D. Smith, *Coord. Chem. Rev.*, 2006, **250**, 3068.
8 L. Fabbrizzi, M. Licchelli and A. Taglietti, *Dalton Trans.*, 2003, 3471.
9 A. Ojida, Y. Mito-oka, M. a. Inoue and I. Hamachi, *J. Am. Chem. Soc.*, 2002, **124**, 6256.
10 D. H. Lee, J. H. Im, S. U. Son, Y. K. Chung and J. I. Hong, *J. Am. Chem. Soc.*, 2003, **125**, 7752.
11 A. Ojida, Y. Mito-oka, K. Sada and I. Hamachi, *J. Am. Chem. Soc.*, 2004, **126**, 2454.
12 A. Ojida, H. Nonaka, Y. Miyahara, S. Tamaru, K. Sada and I. Hamachi, *Angew. Chem., Int. Ed.*, 2006, **45**, 5518.
13 M. J. McDonough, A. J. Reynolds, W. Y. G. Lee and K. A. Jolliffe, *Chem. Commun.*, 2006, **2006**, 2971.
14 H. N. Lee, Z. Xu, S. K. Kim, K. M. K. Swamy, Y. Kim, S. J. Kim and J. Yoon, *J. Am. Chem. Soc.*, 2007, **129**, 3828.
15 H. W. Rhee, C. R. Lee, S. H. Cho, M. R. Song, M. Cashel, H. E. Choy, Y. J. Seok and J. I. Hong, *J. Am. Chem. Soc.*, 2008, **130**, 784.

16 I. S. Shin, S. W. Bae, H. Kim and J. I. Hong, *Anal. Chem.*, 2010, **82**, 8259.
17 H. T. Ngo, X. Liu and K. A. Jollife, *Chem. Soc. Rev.*, 2012, **41**, 4928.
18 Y. Kurishita, T. Kohira, A. Ojida and I. Hamachi, *J. Am. Chem. Soc.*, 2010, **132**, 13290.
19 (*a*) X. J. Peng, F. L. Song, E. H. Lu, Y. N. Wang, W. Zhou, J. L. Fan and Y. L. Gao, *J. Am. Chem. Soc.*, 2005, **127**, 4170; (*b*) L. Tolosa, K. Nowaczyk and J. Lakowicz, *An Introduction to Laser Spectroscopy*, Kluwer, New York, 2nd edn, 2002; (*c*) Z. Zhang and S. Achilefu, *Org. Lett.*, 2004, **6**, 2067; (*d*) J. F. Wang and Y. Pang, *RSC Adv.*, 2013, **3**, 10208.
20 (*a*) M. Taki, J. L. Wolford and T. V. O'Halloran, *J. Am. Chem. Soc.*, 2004, **126**, 712; (*b*) R. Hu, J. Feng, D. H. Hu, S. Q. Wang, S. Y. Li, Y. Li and G. Q. Yang, *Angew. Chem., Int. Ed.*, 2010, **49**, 4915; (*c*) J. S. Wu, W. M. Liu, J. C. Ge, H. Y. Zhang and P. F. Wang, *Chem. Soc. Rev.*, 2011, **40**, 3483; (*d*) Z. Xu, L. Xu, J. Zhou, Y. F. Xu, W. P. Zhu and X. H. Qian, *Chem. Commun.*, 2012, **48**, 10871; (*e*) T. Kim, H. J. Kang, G. Han, S. J. Chung and Y. Kim, *Chem. Commun.*, 2009, 5985; (*f*) J. F. Wang, Y. B. Li, E. Duah, S. Paruchuri, D. M. Zhou and Y. Pang, *J. Mater. Chem. B*, 2014, **2**, 2008.
21 J. F. Wang, W. H. Chen, X. M. Liu, C. Wesdemiotis and Y. Pang, *J. Mater. Chem. B*, 2014, **2**, 3349.
22 (*a*) W. Chen, Y. Xing and Y. Pang, *Org. Lett.*, 2011, **13**, 1262; (*b*) The sensor **1b-Zn** was found to respond also to HADP in ethanol solution.